

Accepted Manuscript

Title: Laser-induced superhydrophobic grid patterns on PDMS for droplet arrays formation

Author: Bahador Farshchian Javad R. Gatabi Steven M. Bernick Sooyeon Park Gwan-Hyoung Lee Ravindranath Droopad Namwon Kim



PII: S0169-4332(16)32277-2
DOI: <http://dx.doi.org/doi:10.1016/j.apsusc.2016.10.153>
Reference: APSUSC 34247

To appear in: *APSUSC*

Received date: 19-6-2016
Revised date: 21-9-2016
Accepted date: 23-10-2016

Please cite this article as: Bahador Farshchian, Javad R.Gatabi, Steven M.Bernick, Sooyeon Park, Gwan-Hyoung Lee, Ravindranath Droopad, Namwon Kim, Laser-induced superhydrophobic grid patterns on PDMS for droplet arrays formation, Applied Surface Science <http://dx.doi.org/10.1016/j.apsusc.2016.10.153>

This is a PDF file of an unedited manuscript that has been accepted for publication. As a service to our customers we are providing this early version of the manuscript. The manuscript will undergo copyediting, typesetting, and review of the resulting proof before it is published in its final form. Please note that during the production process errors may be discovered which could affect the content, and all legal disclaimers that apply to the journal pertain.

Laser-induced superhydrophobic grid patterns on PDMS for droplet arrays formation

Bahador Farshchian¹, Javad R. Gatabi², Steven M. Bernick¹, Sooyeon Park¹, Gwan-Hyoung Lee³, Ravindranath Droopad^{1,2}, and Namwon Kim^{1,*}

¹*Ingram School of Engineering, Texas State University, San Marcos, TX 78666, USA.*

²*Materials Science, Engineering and Commercialization, Texas State University, San Marcos, TX 78666, USA.*

³*Department of Materials Science and Engineering, Yonsei University, Seoul 03722, Republic of Korea*

E-mail: n_k43@txstate.edu

Highlights

- Superhydrophobic grid patterns were processed on the surface of PDMS using a pulsed nanosecond laser.
- Droplet arrays form instantly on the laser-patterned PDMS with the superhydrophobic grid pattern when the PDMS sample is simply immersed in and withdrawn from water.
- Droplet size can be controlled by controlling the pitch size of superhydrophobic grid and the withdrawal speed.

Abstract

We demonstrate a facile single step laser treatment process to render a polydimethylsiloxane (PDMS) surface superhydrophobic. By synchronizing a pulsed nanosecond laser source with a motorized stage, superhydrophobic grid patterns were written on the surface of PDMS. Hierarchical micro and nanostructures were formed in the irradiated areas while non-irradiated areas were covered by nanostructures due to deposition of ablated particles. Arrays of droplets form spontaneously on the laser-patterned PDMS with superhydrophobic grid pattern when the PDMS sample is simply immersed in and withdrawn from water due to different wetting properties of the irradiated and non-irradiated areas. The effect of withdrawal speed, and pitch size of superhydrophobic grid on the size of formed droplets were investigated experimentally. The droplet size increases initially with increasing the withdrawal speed and then does not change significantly beyond certain points. Moreover, larger droplets are formed by increasing the pitch size of the superhydrophobic grid. The droplet arrays formed on the laser-patterned PDMS with wettability contrast can be used potentially for patterning of particles, chemicals, and bio-molecules and also for cell screening applications.

Keywords: laser ablation, superhydrophobic grid, PDMS, droplet arrays, moderate wettability contrast.

1. Introduction

The wetting property of a surface is a function of both surface chemistry and surface topography [1]. Recently, superhydrophobic surfaces defined as surfaces with a static contact angle larger than 150° and a sliding angle less than 10° have attracted extensive attention in virtue of their potential applications for self-cleaning surfaces, anti-icing, anti-fouling, anti-corrosion, and drag reduction in microfluidics [2-6]. Wetting behavior on a rough surface is usually described by the well-established Wenzel [7] or Cassie-Baxter [8] models. In the Wenzel model, the liquid fills the surface structures completely, leading to pinning of droplets on the rough surface (sticky condition). While in the Cassie-Baxter model, the liquid sits only on top of the surface structures and air is trapped between the liquid and the rough surface, which results in a small contact area and a low friction between the droplet and surface, and consequently a low sliding angle (slippery condition).

Among the materials which have been used for fabrication of superhydrophobic surfaces, silicon-based elastomer, polydimethylsiloxane (PDMS), offers various advantages. Because of its water repellency and high electrical resistance, PDMS is a suitable material to replace glass and porcelain in housing and high voltage insulators [9]. PDMS also has been widely used in soft lithography for the fabrication of microfluidic devices because of its non-toxicity, optical transparency, and flexibility [10, 11]. Since the PDMS surface is intrinsically hydrophobic, enhancing its surface roughness can potentially turn its surface superhydrophobic. Various techniques have been employed to render the surface of PDMS superhydrophobic. Sun *et al.* replicated a lotus leaf as a natural superhydrophobic template on the PDMS surface by nanocasting to obtain a superhydrophobic surface [12]. Tserepi *et al.* treated a PDMS surface with sulfur hexafluoride (SF_6) plasma to form high aspect ratio columnar-like nanostructures and

subsequently coated its surface with fluorocarbon using octafluorocyclobutane (C_4F_8) plasma to enhance the hydrophobicity [13]. Cortese *et al.* used a two-step process to create a hierarchical double scale roughness on the surface of PDMS to acquire a superhydrophobic state. Firstly, micropillars were formed on a PDMS surface by replicating a micropatterned SU-8 master onto PDMS and then nanoposts were formed on the top of the micropillars by exposing the micropatterned PDMS to tetrafluoromethane (CF_4) plasma [14]. Nanostructures were also formed on the PDMS surface to achieve superhydrophobicity by a surface-initiated polymerization and acidic treatment using sulfuric or hydrofluoric acid [15, 16]. In addition, pulsed laser irradiation has been used to manipulate surface properties of PDMS [17-22] and fabricate superhydrophobic PDMS surfaces [23-26]. Pulsed laser treatment has shown repeatable, precise, and controllable surface modifications on a variety of materials such as metals [27-30], polymers [9, 23-26, 31, 32], silicon [33, 34], ceramics [35, 36], and composite [37]. Moreover, the desired patterns can be readily written on a surface without any contamination by directly exposing the surface to laser in a computer-controlled system [38].

In this study, we used a nanosecond pulsed laser system to create superhydrophobic grid patterns on a PDMS surface for spontaneous formation of water droplet arrays. By synchronizing the laser light source with a motorized stage, the superhydrophobic grids were directly written on the PDMS surface. The surface topography of the patterned PDMS was investigated by scanning electron microscope (SEM) and the contact angles of water droplets on the treated PDMS surface were measured at different time intervals after fabrication until superhydrophobicity was achieved. We demonstrate that laser-patterned PDMS with superhydrophobic grids can be used as an effective tool for the formation of small droplet arrays by simply immersing and withdrawing the laser-patterned PDMS in and out of water. The size of formed droplets can be

controlled with the withdrawal speed, and pitch size of grids. Such microarrays of the droplets can be used as templates for the patterning of particles, chemicals, and any compound in the aqueous solutions. Also, cells can be encapsulated in the arrays of microdroplets and hydrogels for cell screening and for cell culturing in a 3D microenvironment [39-41].

2. Experimental

Sylgard 184 (Dow Corning Corp., MI) silicone rubber base and curing agent were mixed at a 10:1 mass ratio. In order to remove air bubbles, the mixture was vacuumed for 20 min. After removing air bubbles, the PDMS was poured into a glass petri dish up to a height of 3 mm, vacuumed again and cured at 65 ° C for 4 h in a convection oven. The cured PDMS was peeled off from the glass petri dish and cut into 3 cm × 8 cm rectangular pieces using a razor blade. Figure 1a shows the experimental setup of the laser-patterning system used in this experiment. The laser source used was an excimer laser system (COMpexPRO 201, Coherent Inc., CA) which generates 25 ns pulsed laser at 248 nm wavelength with the maximum pulse repetition rate of 10 Hz and maximum pulse energy of 700 mJ. The pulsed laser was guided and focused on the PDMS surface using a mirror and two lenses. To control the size of the beam adjustable apertures were used. The desired superhydrophobic patterns were directly written on the PDMS surface by programming a motorized x-y stage and synchronizing the laser system with the stage. The scanning speed, pulse frequency, laser fluence, and overlapping ratio were 0.5 mm/s, 10 Hz, 5 J/cm², and 50%, respectively. 5 mm × 5 mm square superhydrophobic patterns, superhydrophobic TEXAS STATE patterns, superhydrophobic grid patterns with the pitch sizes of 0.5, 1, and 2 mm, and 2.5 cm × 2.5 cm superhydrophobic patterns enclosing a 5 mm × 5 mm untreated area at the center were written on the PDMS surface. Three samples were prepared for each of those patterns. Figure 1b shows a photo of a PDMS sample attached to the x-y stage during writing TEXAS STATE pattern on it. A photo of a PDMS sample with superhydrophobic

grid pattern with pitch size of 1mm after laser patterning is also demonstrated in figure 1c. Morphology of the laser-patterned PDMS was observed by SEM (Helios Nano Lab 400, FEI, OR). Surface roughness and 3D topography image of the laser-patterned PDMS were acquired using a stylus surface profiler (KLA-Tencor, P-7, CA). To study aging of the laser-treated PDMS, static contact angles of 5 μ L water droplets resting on the laser-treated PDMS surface were measured at different time intervals using a contact angle analyzer (Falcon, First Ten Angstroms Inc., VA). Five measurements were taken to calculate the average contact angle at each time interval. To measure the sliding angle of water droplet on a superhydrophobic PDMS surface, a manual goniometer (GN05, Thorlabs Inc, NJ) was used. Five measurements of the sliding angle for 5 μ L water droplets were performed. In order to form arrays of droplets, the laser-patterned PDMS with a superhydrophobic grid pattern was immersed in a beaker full of water and then immediately withdrawn. A lifter robot, capable of immersing the laser-patterned PDMS samples into water and withdrawing it out of water at a constant speed, was built in order to control the withdrawal speed of the PDMS samples. We measured the size of droplets formed on the superhydrophobic grid patterns with the pitch sizes of 0.5, 1, and 2 mm as a function of different withdrawal speeds of 5.7, 14.5, 30, 43.5, and 55.7 cm/s. Three measurements were conducted at each withdrawal speed. The images of the droplets formed on the laser-patterned PDMS were then acquired using an optical microscope equipped with a 2.5 \times objective. The diameters of the droplets parallel and vertical to the withdrawal direction were measured and averaged to calculate each droplet diameter.

3. Results and discussions

During the laser irradiation, high-temperature and high-pressure plasma forms on the PDMS surface as a result of the interaction between the laser light and PDMS. As the plasma

expands and bursts out of focal spot shock waves form. The shock waves remove the ablated materials and form dual-scale surface roughness on PDMS [26, 42, 43]. Figures 2a and b show the SEM images for the top and tilted views of the laser-treated PDMS, respectively. The inset in figure 2a shows a magnified image of the top view of the surface. After the samples were irradiated with the laser, the surface of PDMS became considerably rough, forming irregular multi-scale structures consisting of microstructures with sizes smaller than 20 μm covered with tens or hundreds of nanometer structures. The root-mean-square (rms) roughness which is the standard deviation of the height values of surface structures was measured by the stylus profiler to be 1.56 μm .

Figure 3 shows the evolution of the static contact angle of a water droplet on the laser-treated PDMS surface at different time intervals after laser treatment of the PDMS. The static contact angle decreases drastically to $38 \pm 2^\circ$ compared to the untreated PDMS, $111 \pm 2^\circ$, and then increases gradually with time, eventually reaching $154 \pm 2^\circ$ after 5 hours, causing the surface to achieve a superhydrophobic state. The contact angle evolution can be approximated with an exponential growth curve, $\theta/\theta_{eq} = 1 - e^{-t/\lambda}$ where θ_{eq} is the maximum contact angle toward which the contact angles converge and λ is a time constant, which represents the time at which 63.2% of the maximum contact angle value is reached. The values of θ_{eq} and λ are 154° and 1.15 hr, respectively. The value of sliding angle of water droplet on the laser-treated PDMS surface was measured to be $4 \pm 2^\circ$.

As a result of the laser-induced ablation, the PDMS surface is significantly roughened. Furthermore, it causes formation of oxide groups [23, 44], decomposition of PDMS, and formation of crystalline silicon and amorphous carbon [19-22], which drastically increase the surface energy. At the initial stage after laser irradiation, a combination of high surface energy

and high surface roughness causes the noticeable drop of the contact angle. However, the surface energy decreases and hydrophobicity recovers gradually due to the reorientation of surface oxide groups and/or immigration of low molecular weight (LMW) silicone generated during laser treatment from below the surface towards the surface [22, 44]. Hydrophobic recovery of PDMS exposed to the plasma, UV/ozone and corona discharge has also been reported [45-49]. Close inspection of SEM images revealed no discernible difference of surface topography between the laser-treated PDMS samples immediately and 5 hours after treatment. The surface chemistry recovery coupled with high surface roughness causes the interaction of a water droplet and the laser-treated PDMS to be limited, therefore facilitating conditions for extreme water repellency. The inset in figure 3 shows a water droplet on a laser-irradiated area of PDMS after 5 hrs. The laser-irradiated area appears dark compared to the transparent non-irradiated area because of enhanced surface roughness and the water droplet beads up on the superhydrophobic surface. Superhydrophobic grid patterns with different pitch sizes of 0.5, 1, and 2 mm were written on the PDMS surface. Figure 4a shows a grid pattern with 0.5 mm pitch written on PDMS by the laser irradiation. The magnified images of the irradiated and non-irradiated areas of PDMS surface are shown in figures 4b and e, respectively. Irregular hierarchical micro and nanostructures form in the laser-irradiated grid (LIG) area (figure 4b) by the laser ablation. In contrast, the non-irradiated cell (NIC) area (figure 4e) is partially covered by nanostructures because of the deposition of ablated particles on its surface. The ablation of PDMS in the LIG areas causes a height difference of about 10 μm between the top surface of the cells and the bottom surface of the grids (figures 4c and d). Using the laser-patterned PDMS samples with a 2.5 cm \times 2.5 cm superhydrophobic LIG area enclosing a 5 mm \times 5 mm hydrophobic NIC area at the center, the static contact angle of water droplets on the NIC areas was measured 5 hours after fabrication.

The measured static contact angle was $121 \pm 2^\circ$, which achieves the moderate wettability contrast along with the LIC areas of $154 \pm 2^\circ$ contact angle.

Laser-patterned PDMS samples with the moderate wettability contrast were used as templates to form droplet arrays 5 hours after their fabrication to ensure that the LIG areas reached the superhydrophobic state. The laser-patterned PDMS was simply immersed in and withdrawn vertically from water to form droplet arrays. When the PDMS sample was fully immersed in water, the LIG area exhibited a mirror-like sheen caused by light reflection from the thin layer of air trapped on the superhydrophobic surface [50]. Water contacting the LIG areas has a Cassie-Baxter state, in which it only contacts the peaks of the hierarchical micro and nanostructures. Whereas, water contacting the NIC area has a Wenzel state, in which the whole surface is completely wetted during immersion (figure 5a). When the laser-patterned PDMS is lifted vertically out of water, two areas experience different frictional drags, i.e. the higher frictional drag on the NIC surface and the lower frictional drag on the LIG surface. The trapped air on the superhydrophobic LIG area results in reduced frictional drag compared to the neighboring NIC areas [51]. The surface condition varies alternatively across the LIG and NIC areas. As the result of this difference in frictional drag, the contact lines on the LIG surface moves faster than the ones on the NIC surface during withdrawal from water (figure 5b). The velocity differences of the contact lines eventually leads to pinching off water covering the NIC areas and results in spontaneous droplet formation on their surface (figure 5c).

Droplet arrays formed on the laser-patterned PDMS when PDMS was immersed in and withdrawn from water at a speed of 55.7 cm/s are demonstrated in figures 6a-d. Following withdrawal, the LIG areas (the dark areas) remain dry and the NIC area (the transparent areas) become partially wet. Figure 7 shows the graph in which the droplet sizes versus withdrawal

speed for grids with different pitch sizes are plotted. The droplet size increases initially as the withdrawal speed increases for all the sizes of the grid pitches and then does not significantly increase beyond a certain point. At lower withdrawal speeds the contact lines on NIC areas have more time to sweep over the surface before pinch off occurs, therefore less water will remain on top of them after pinch off. At a certain speed as the grid pitch size increases, i.e. the area of the NIC increases, the size of droplets increase. Increasing the area of the cells causes the Wenzel contact area between water and NIC surface during immersion to increase. Thus, more water will remain on top of the NIC as the sample is withdrawn from water and pinch-off happens.

There have been reports for droplet arrays formation on surfaces with extreme wettability contrast (superhydrophobic areas vs. superhydrophilic areas), which were often fabricated using intricate multistep processes [40, 52, 53]. In this research, surfaces with moderate wettability contrast (hydrophobic areas vs. superhydrophobic areas) were fabricated in a single step by writing superhydrophobic patterns on an intrinsically hydrophobic material without any further chemical treatment. Unlike the platforms with extreme wettability contrast in which the surfaces of superhydrophilic areas become fully wet when a liquid is applied to them, the hydrophobic areas (NIC) surrounded by superhydrophobic areas (LIG) on the platform that we have designed and fabricated by laser patterning only get wet partially. This happens due to the fact that the contact lines of the applied liquid can move on the hydrophobic areas of the platform with moderate wettability contrast, while the contact lines are pinned in the superhydrophilic areas of the platform with extreme wettability contrast. This allows controlling the size of the droplets not only by the grid size, but also by the withdrawal speed as discussed above. The laser-patterned PDMS with superhydrophobic grid patterns can also be used potentially as a master mold for the mass production of superhydrophobic grids. The minimum feature size that can be replicated by

casting is 20 nm [54]. Yoon *et al.* has shown a positive replica of the superhydrophobic laser-treated PDMS, which is replicated on PDMS, still has superhydrophobic properties [26]. Laser treatment of PDMS described in this work can also be applied for other applications including passive valves in microfluidics [55], droplet-driven transports on surface microfluidics [56], transport of fluids between component chips in modular microfluidic systems [26], superhydrophobic nozzles for contact-free dosage [57], and mixing in microfluidics [58].

4. Conclusions

As a result of the laser-induced ablation of PDMS, the surface of PDMS becomes significantly rougher forming hierarchical micro and nanostructures. This combined with a low surface energy of PDMS, which is reinstated five hours after laser treatment will impart extreme water repellency to the surface. Therefore, no second chemical coating step is required and superhydrophobicity state can be achieved merely using the laser treatment. Superhydrophobic grid patterns with different pitch sizes of 0.5 mm, 1 mm, and 2mm were directly written on the surface of PDMS by synchronizing the laser system with an x-y motorized stage. Droplet arrays formed on the laser-patterned PDMS when it was immersed in and withdrawn from water. As the laser-patterned PDMS with superhydrophobic grid is withdrawn from water the contact lines on laser-irradiated areas move faster than the ones on non-irradiated areas which eventually leads to pinching off water covering the non-irradiated areas resulting in instantaneous droplet formation on their surface. The effect of withdrawal speed, and pitch size of superhydrophobic grids written on the surface of PDMS on the droplet size were investigated. Initial increase of withdrawal speed causes droplet size to increase but its further increase over certain values does not significantly change the droplet size. At lower withdrawal speeds the contact line on the laser-irradiated area has more time to sweep over the surface, therefore less water will remain on

top of its surface after pinch-off. At a certain withdrawal speed, the droplet size increases as the pitch size of superhydrophobic grid increases. The increase in the pitch size of the superhydrophobic grid causes the Wenzel contact area between top of the laser-irradiated area and water during immersion increases. As a result, more water will remain on top of its surface after pinch-off occurs.

Acknowledgment

This research was supported by Texas State University research fund, International Research & Development Program of the National Research Foundation of Korea (NRF) funded by the Ministry of Science, ICT and Future Planning of Korea (2016K1A3A1A25003573), the Human Resources Program in Energy Technology of the Korea Institute of Energy Technology Evaluation and Planning (KETEP), granted financial resource from the Ministry of Trade, Industry & Energy of Korea (No.20154010200810), and in part by the Yonsei University Future-leading Research Initiative.

Reference

- [1] A. Lafuma and D. Quere, "Superhydrophobic states," *Nature Materials*, vol. 2, pp. 457-460, Jul 2003.
- [2] B. Bhushan, Y. C. Jung, and K. Koch, "Self-Cleaning Efficiency of Artificial Superhydrophobic Surfaces," *Langmuir*, vol. 25, pp. 3240-3248, Mar 3 2009.
- [3] C. Peng, S. Xing, Z. Yuan, J. Xiao, C. Wang, and J. Zeng, "Preparation and anti-icing of superhydrophobic PVDF coating on a wind turbine blade," *Applied Surface Science*, vol. 259, pp. 764-768, Oct 15 2012.
- [4] J. Chapman and F. Regan, "Nanofunctionalized Superhydrophobic Antifouling Coatings for Environmental Sensor ApplicationsuAdvancing Deployment with Answers from Nature," *Advanced Engineering Materials*, vol. 14, pp. B175-B184, Apr 2012.
- [5] Z. She, Q. Li, Z. Wang, L. Li, F. Chen, and J. Zhou, "Researching the fabrication of anticorrosion superhydrophobic surface on magnesium alloy and its mechanical stability and durability," *Chemical Engineering Journal*, vol. 228, pp. 415-424, Jul 15 2013.
- [6] O. I. Vinogradova and A. L. Dubov, "Superhydrophobic textures for microfluidics," *Mendelevov Communications*, vol. 22, pp. 229-236, Sep-Oct 2012.
- [7] R. N. Wenzel, "Resistance of solid surfaces to wetting by water," *Industrial and Engineering Chemistry*, vol. 28, pp. 988-994, 1936 1936.
- [8] A. B. D. Cassie and S. Baxter, "Wettability of porous surfaces," *Transactions of the Faraday Society*, vol. 40, pp. 0546-0550, 1944 1944.
- [9] M. H. Jin, X. J. Feng, J. M. Xi, J. Zhai, K. W. Cho, L. Feng, *et al.*, "Super-hydrophobic PDMS surface with ultra-low adhesive force," *Macromolecular Rapid Communications*, vol. 26, pp. 1805-1809, Nov 14 2005.
- [10] M. A. Unger, H. P. Chou, T. Thorsen, A. Scherer, and S. R. Quake, "Monolithic microfabricated valves and pumps by multilayer soft lithography," *Science*, vol. 288, pp. 113-116, Apr 7 2000.
- [11] J. C. McDonald, D. C. Duffy, J. R. Anderson, D. T. Chiu, H. K. Wu, O. J. A. Schueller, *et al.*, "Fabrication of microfluidic systems in poly(dimethylsiloxane)," *Electrophoresis*, vol. 21, pp. 27-40, Jan 2000.
- [12] M. H. Sun, C. X. Luo, L. P. Xu, H. Ji, O. Y. Qi, D. P. Yu, *et al.*, "Artificial lotus leaf by nanocasting," *Langmuir*, vol. 21, pp. 8978-8981, Sep 13 2005.
- [13] A. D. Tserepi, M. E. Vlachopoulou, and E. Gogolides, "Nanotexturing of poly(dimethylsiloxane) in plasmas for creating robust super-hydrophobic surfaces," *Nanotechnology*, vol. 17, pp. 3977-3983, Aug 14 2006.

- [14] B. Cortese, S. D'Amone, M. Manca, I. Viola, R. Cingolani, and G. Gigli, "Superhydrophobicity due to the hierarchical scale roughness of PDMS surfaces," *Langmuir*, vol. 24, pp. 2712-2718, Mar 18 2008.
- [15] T. Qian, Y. Li, Y. Wu, B. Zheng, and H. Ma, "Superhydrophobic poly(dimethylsiloxane) via surface-initiated polymerization with ultralow initiator density," *Macromolecules*, vol. 41, pp. 6641-6645, Sep 23 2008.
- [16] E. P. T. de Givenchy, S. Amigoni, C. Martin, G. Andrada, L. Caillier, S. Geribaldi, *et al.*, "Fabrication of Superhydrophobic PDMS Surfaces by Combining Acidic Treatment and Perfluorinated Monolayers," *Langmuir*, vol. 25, pp. 6448-6453, Jun 2 2009.
- [17] P. A. Atanasov, N. E. Stankova, N. N. Nedyalkov, N. Fukata, D. Hirsch, B. Rauschenbach, *et al.*, "Fs-laser processing of medical grade polydimethylsiloxane (PDMS)," *Applied Surface Science*, vol. 374, pp. 229-234, Jun 2016.
- [18] P. A. Atanasov, N. N. Nedyalkov, E. I. Valova, Z. S. Georgieva, S. A. Armyanov, K. N. Kolev, *et al.*, "Fs-laser processing of polydimethylsiloxane," *Journal of Applied Physics*, vol. 116, p. 4, Jul 2014.
- [19] N. E. Stankova, P. A. Atanasov, R. G. Nikov, R. G. Nikov, N. N. Nedyalkov, T. R. Stoyanov, *et al.*, "Optical properties of polydimethylsiloxane (PDMS) during nanosecond laser processing," *Applied Surface Science*, vol. 374, pp. 96-103, Jun 2016.
- [20] N. E. Stankova, P. A. Atanasov, N. N. Nedyalkov, T. R. Stoyanov, K. N. Kolev, E. I. Valova, *et al.*, "fs- and ns-laser processing of polydimethylsiloxane (PDMS) elastomer: Comparative study," *Applied Surface Science*, vol. 336, pp. 321-328, May 2015.
- [21] P. A. Atanasov, N. E. Stankova, N. N. Nedyalkov, T. R. Stoyanov, R. G. Nikov, N. Fukata, *et al.*, "Properties of ns-laser processed polydimethylsiloxane (PDMS)" *Journal of Physics: Conference series* vol. 700, p. 012023, 2016.
- [22] C. Dupas-Bruzek, O. Robbe, A. Addad, S. Turrell, and D. Derozier, "Transformation of medical grade silicone rubber under Nd:YAG and excimer laser irradiation: First step towards a new miniaturized nerve electrode fabrication process," *Applied Surface Science*, vol. 255, pp. 8715-8721, Aug 2009.
- [23] M. T. Khorasani, H. Mirzadeh, and P. G. Sammes, "Laser induced surface modification of polydimethylsiloxane as a super-hydrophobic material," *Radiation Physics and Chemistry*, vol. 47, pp. 881-888, Jun 1996.
- [24] S. van Pelt, A. Frijns, R. Mandampambil, and J. den Toonder, "Local wettability tuning with laser ablation redeposits on PDMS," *Applied Surface Science*, vol. 303, pp. 456-464, Jun 1 2014.
- [25] J. Yong, F. Chen, Q. Yang, D. Zhang, H. Bian, G. Du, *et al.*, "Controllable Adhesive Superhydrophobic Surfaces Based on PDMS Microwell Arrays," *Langmuir*, vol. 29, pp. 3274-3279, Mar 12 2013.

- [26] T. O. Yoon, H. J. Shin, S. C. Jeoung, and Y.-I. Park, "Formation of superhydrophobic poly(dimethylsiloxane) by ultrafast laser-induced surface modification," *Optics Express*, vol. 16, pp. 12715-12725, Aug 18 2008.
- [27] S. Moradi, S. Kamal, P. Englezos, and S. G. Hatzikiriakos, "Femtosecond laser irradiation of metallic surfaces: effects of laser parameters on superhydrophobicity," *Nanotechnology*, vol. 24, Oct 18 2013.
- [28] R. Jagdheesh, B. Pathiraj, E. Karatay, G. R. B. E. Roemer, and A. J. H. in't Veldt, "Laser-Induced Nanoscale Superhydrophobic Structures on Metal Surfaces," *Langmuir*, vol. 27, pp. 8464-8469, Jul 5 2011.
- [29] A. Y. Vorobyev and C. Guo, "Multifunctional surfaces produced by femtosecond laser pulses," *Journal of Applied Physics*, vol. 117, Jan 21 2015.
- [30] A.-M. Kietzig, S. G. Hatzikiriakos, and P. Englezos, "Patterned Superhydrophobic Metallic Surfaces," *Langmuir*, vol. 25, pp. 4821-4827, Apr 21 2009.
- [31] R. M. Wagterveld, C. W. J. Berendsen, S. Bouaidat, and J. Jonsmann, "Ultralow hysteresis superhydrophobic surfaces by excimer laser modification of SU-8," *Langmuir*, vol. 22, pp. 10904-10908, Dec 19 2006.
- [32] J. Yong, Q. Yang, F. Chen, D. Zhang, G. Du, H. Bian, *et al.*, "Superhydrophobic PDMS surfaces with three-dimensional (3D) pattern-dependent controllable adhesion," *Applied Surface Science*, vol. 288, pp. 579-583, Jan 1 2014.
- [33] M. Barberoglou, V. Zorba, E. Stratakis, E. Spanakis, P. Tzanetakis, S. H. Anastasiadis, *et al.*, "Bio-inspired water repellent surfaces produced by ultrafast laser structuring of silicon," *Applied Surface Science*, vol. 255, pp. 5425-5429, Mar 1 2009.
- [34] T. Baldacchini, J. E. Carey, M. Zhou, and E. Mazur, "Superhydrophobic surfaces prepared by microstructuring of silicon using a femtosecond laser," *Langmuir*, vol. 22, pp. 4917-4919, May 23 2006.
- [35] R. Jagdheesh, "Fabrication of a Superhydrophobic Al₂O₃ Surface Using Picosecond Laser Pulses," *Langmuir*, vol. 30, pp. 12067-12073, Oct 14 2014.
- [36] J. Yong, F. Chen, Q. Yang, Y. Fang, J. Huo, and X. Hou, "Femtosecond laser induced hierarchical ZnO superhydrophobic surfaces with switchable wettability," *Chemical Communications*, vol. 51, pp. 9813-9816, 2015 2015.
- [37] A. Milionis, D. Fragouli, F. Brandi, I. Liakos, S. Barroso, R. Ruffilli, *et al.*, "Superhydrophobic/superoleophilic magnetic elastomers by laser ablation," *Applied Surface Science*, vol. 351, pp. 74-82, Oct 1 2015.
- [38] F. Chen, D. Zhang, Q. Yang, J. Yong, G. Du, J. Si, *et al.*, "Bioinspired Wetting Surface via Laser Microfabrication," *Acs Applied Materials & Interfaces*, vol. 5, pp. 6777-6792, Aug 14 2013.

- [39] E. Ueda, F. L. Geyer, V. Nedashkivska, and P. A. Levkin, "Droplet Microarray: facile formation of arrays of microdroplets and hydrogel micropads for cell screening applications," *Lab on a Chip*, vol. 12, pp. 5218-5224, 2012 2012.
- [40] F. L. Geyer, E. Ueda, U. Liebel, N. Grau, and P. A. Levkin, "Superhydrophobic-Superhydrophilic Micropatterning: Towards Genome-on-a-Chip Cell Microarrays," *Angewandte Chemie-International Edition*, vol. 50, pp. 8424-8427, 2011 2011.
- [41] A. A. Popova, S. M. Schillo, K. Demir, E. Ueda, A. Nesterov-Mueller, and P. A. Levkin, "Droplet-Array (DA) Sandwich Chip: A Versatile Platform for High-Throughput Cell Screening Based on Superhydrophobic-Superhydrophilic Micropatterning," *Advanced Materials*, vol. 27, pp. 5217-5222, Sep 16 2015.
- [42] J. Yong, F. Chen, Q. Yang, G. Du, H. Bian, D. Zhang, *et al.*, "Rapid Fabrication of Large-Area Concave Micro lens Arrays on PDMS by a Femtosecond Laser," *Acs Applied Materials & Interfaces*, vol. 5, pp. 9382-9385, Oct 9 2013.
- [43] B. Hao, H. Liu, F. Chen, Q. Yang, P. Qu, G. Du, *et al.*, "Versatile route to gapless microlens arrays using laser-tunable wet-etched curved surfaces," *Optics Express*, vol. 20, pp. 12939-12948, Jun 4 2012.
- [44] S. Armyanov, N. E. Stankova, P. A. Atanasov, E. Valova, K. Kolev, J. Georgieva, *et al.*, "XPS and mu-Raman study of nanosecond-laser processing of poly(dimethylsiloxane) (PDMS)," *Nuclear Instruments & Methods in Physics Research Section B-Beam Interactions with Materials and Atoms*, vol. 360, pp. 30-35, Oct 2015.
- [45] J. L. Fritz and M. J. Owen, "Hydrophobic recovery of plasma-treated polydimethylsiloxane," *Journal of Adhesion*, vol. 54, pp. 33-45, 1995 1995.
- [46] A. Olah, H. Hillborg, and G. J. Vancso, "Hydrophobic recovery of UV/ozone treated poly(dimethylsiloxane): adhesion studies by contact mechanics and mechanism of surface modification," *Applied Surface Science*, vol. 239, pp. 410-423, Jan 31 2005.
- [47] H. Hillborg and U. W. Gedde, "Hydrophobicity recovery of polydimethylsiloxane after exposure to corona discharges," *Polymer*, vol. 39, pp. 1991-1998, May 1998.
- [48] J. Kim, M. K. Chaudhury, and M. J. Owen, "Hydrophobic recovery of polydimethylsiloxane elastomer exposed to partial electrical discharge," *Journal of Colloid and Interface Science*, vol. 226, pp. 231-236, Jun 2000.
- [49] J. Kim, M. K. Chaudhury, and M. J. Owen, "Hydrophobicity loss and recovery of silicone HV insulation," *Ieee Transactions on Dielectrics and Electrical Insulation*, vol. 6, pp. 695-702, Oct 1999.
- [50] R. Poetes, K. Holtzmann, K. Franze, and U. Steiner, "Metastable Underwater Superhydrophobicity," *Physical Review Letters*, vol. 105, Oct 14 2010.

- [51] G. McHale, M. I. Newton, and N. J. Shirtcliffe, "Immersed superhydrophobic surfaces: Gas exchange, slip and drag reduction properties," *Soft Matter*, vol. 6, pp. 714-719, 2010.
- [52] H. Z. Li, Q. Yang, G. N. Li, M. Z. Li, S. T. Wang, and Y. L. Song, "Splitting a Droplet for Femtoliter Liquid Patterns and Single Cell Isolation," *Acs Applied Materials & Interfaces*, vol. 7, pp. 9060-9065, May 2015.
- [53] Y. K. Lai, L. X. Lin, F. Pan, J. Y. Huang, R. Song, Y. X. Huang, *et al.*, "Bioinspired Patterning with Extreme Wettability Contrast on TiO₂ Nanotube Array Surface: A Versatile Platform for Biomedical Applications," *Small*, vol. 9, pp. 2945-2953, Sep 2013.
- [54] X. M. Zhao, Y. N. Xia, and G. M. Whitesides, "Soft lithographic methods for nanofabrication," *Journal of Materials Chemistry*, vol. 7, pp. 1069-1074, Jul 1997.
- [55] G. Londe, A. Chunder, A. Wesser, L. Zhai, and H. J. Cho, "Microfluidic valves based on superhydrophobic nanostructures and switchable thermosensitive surface for lab-on-a-chip (LOC) systems," *Sensors and Actuators B-Chemical*, vol. 132, pp. 431-438, Jun 16 2008.
- [56] S. Xing, R. S. Harake, and T. Pan, "Droplet-driven transports on superhydrophobic-patterned surface microfluidics," *Lab on a Chip*, vol. 11, pp. 3642-3648, 2011 2011.
- [57] A. Tropmann, L. Tanguy, P. Koltay, R. Zengerle, and L. Riegger, "Completely Superhydrophobic PDMS Surfaces for Microfluidics," *Langmuir*, vol. 28, pp. 8292-8295, Jun 5 2012.
- [58] D. B. Wolfe, J. B. Ashcom, J. C. Hwang, C. B. Schaffer, E. Mazur, and G. M. Whitesides, "Customization of poly(dimethylsiloxane) stamps by micromachining using a femtosecond-pulsed laser," *Advanced Materials*, vol. 15, pp. 62-+, Jan 3 2003.

List of Figures

Figure 1: (a) The experimental setup of the laser-patterning system (b) photo of a PDMS sample attached to the x-y stage during writing TEXAS STATE pattern on it. (c) photo of a PDMS sample with superhydrophobic grid pattern with pitch size of 1mm

Figure 2: SEM pictures, top view and tilted view of the laser-treated PDMS.

Figure 3: Evolution of static contact angle of water droplet on the laser-treated PDMS at different time intervals after fabrication (experimental and theoretical). The insets show a photo of a water droplet on the laser-treated PDMS 5 hours after fabrication.

Figure 4: SEM picture of (a) PDMS sample with superhydrophobic grid pattern when the grid pitch size is 500 μm . (b) LIG: laser-irradiated grid; (c) Surface height map and (d) 3D topography image of the surface. (e) SEM picture of NIC: non-irradiated cell.

Figure 5: Schematic illustrating (a) Wenzel contact and Cassie-Baxter contact on laser-patterned PDMS sample immersed in water (b) contact line movement on LIG: laser-irradiated grid and NIC: non-irradiated cell areas. (c) droplet formation on laser-patterned PDMS with superhydrophobic grid.

Figure 6: (a) Photo of water droplet arrays formed on the laser-patterned PDMS with superhydrophobic grid with pitch size of 1 mm and optical microscope pictures of the droplet arrays formed on the laser-patterned PDMS with superhydrophobic grids with different pitch sizes of (a) 2 mm (b) 1 mm (c) 0.5 mm when the laser-patterned PDMS sample was immersed in and withdrawn from water at speed of 55.7 cm/s.

Figure 7: Droplet size versus withdrawal speed for the droplet arrays formed on laser-patterned PDMS with superhydrophobic grids with pitch sizes of 2 mm, 1 mm and 0.5 mm when PDMS sample was immersed in and withdrawn from water

Figure 1

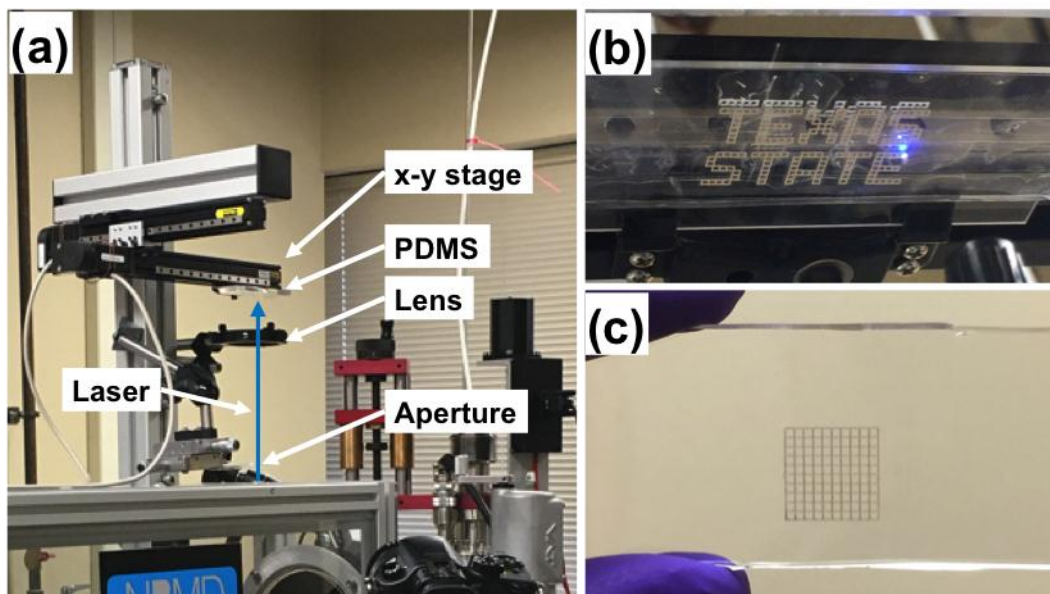


Figure 2

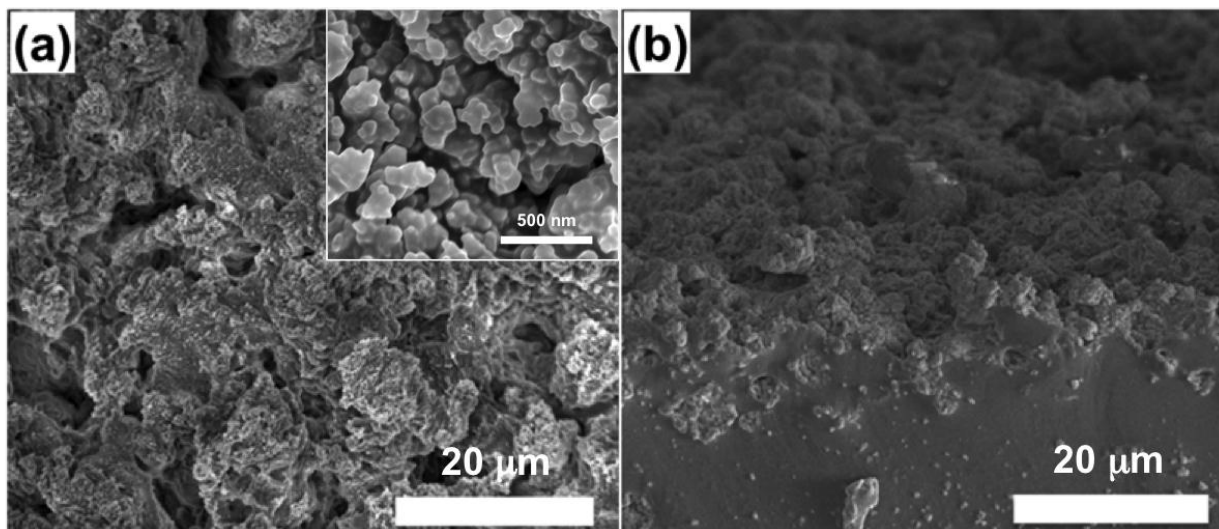


Figure 3

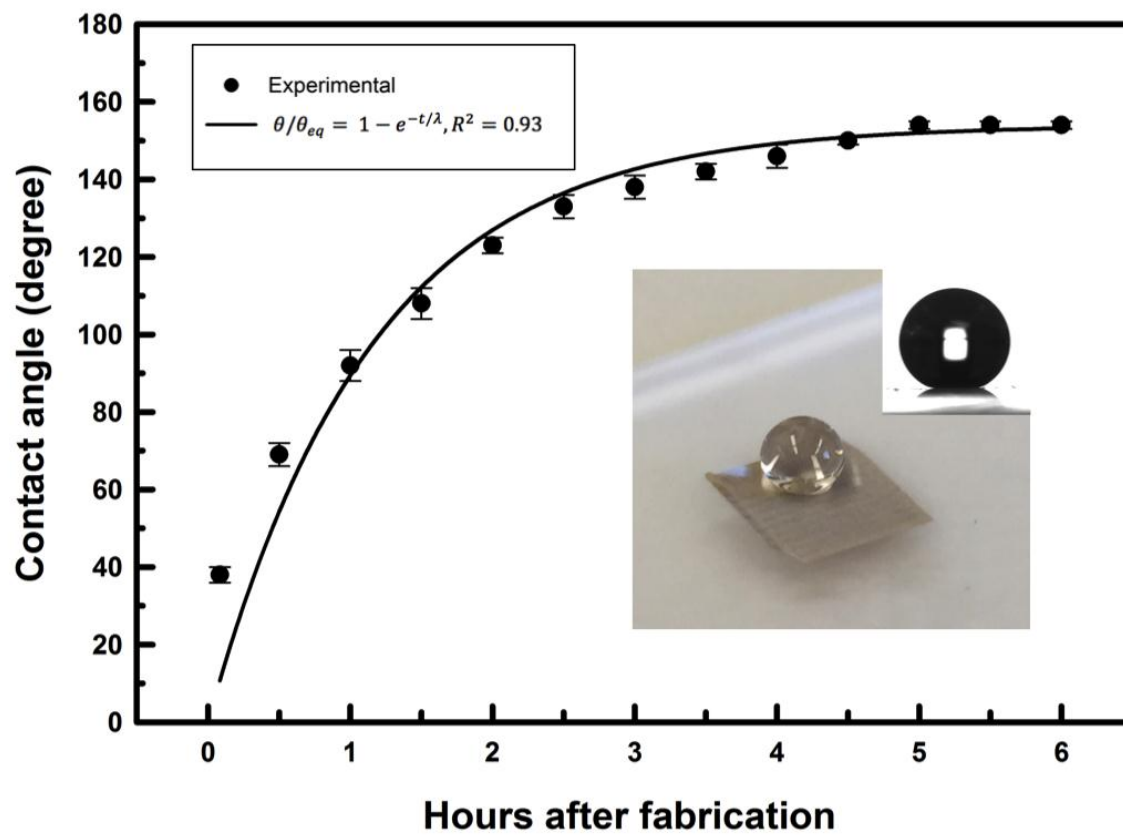


Figure 4

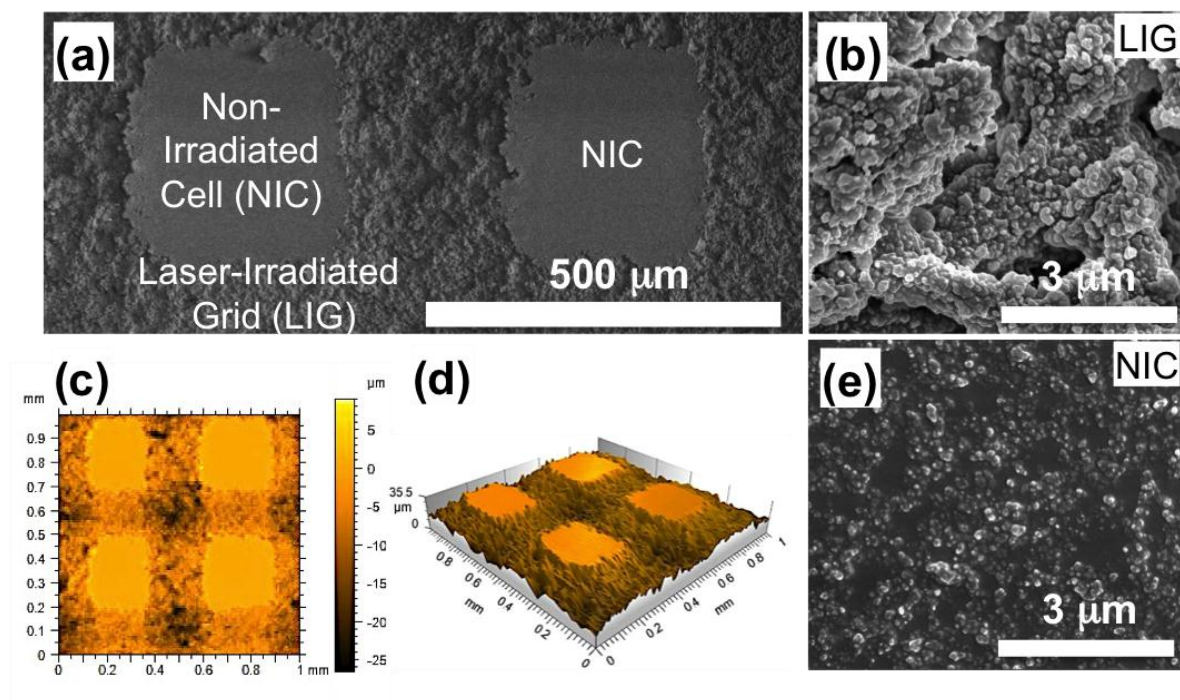


Figure 5

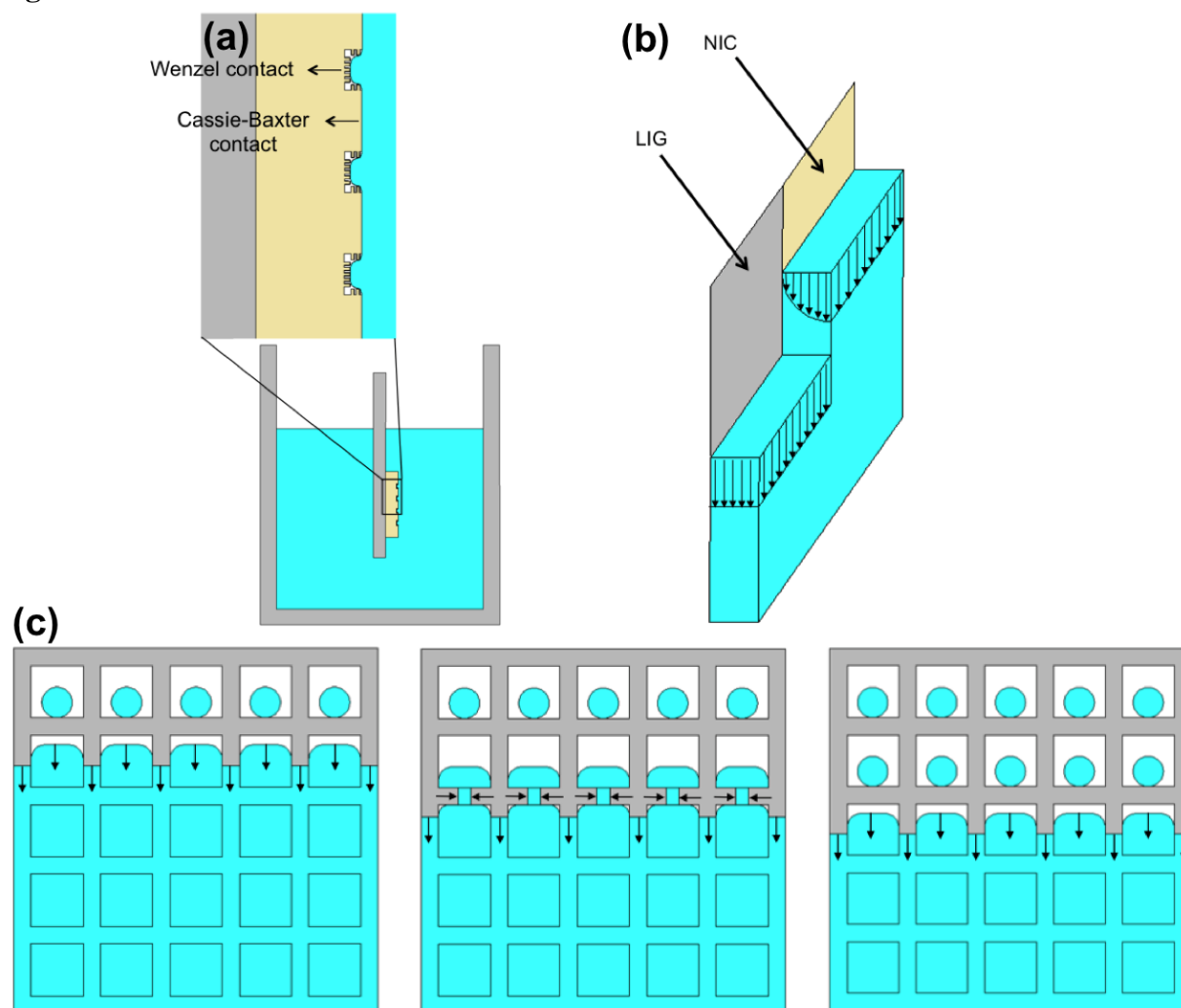


Figure 6

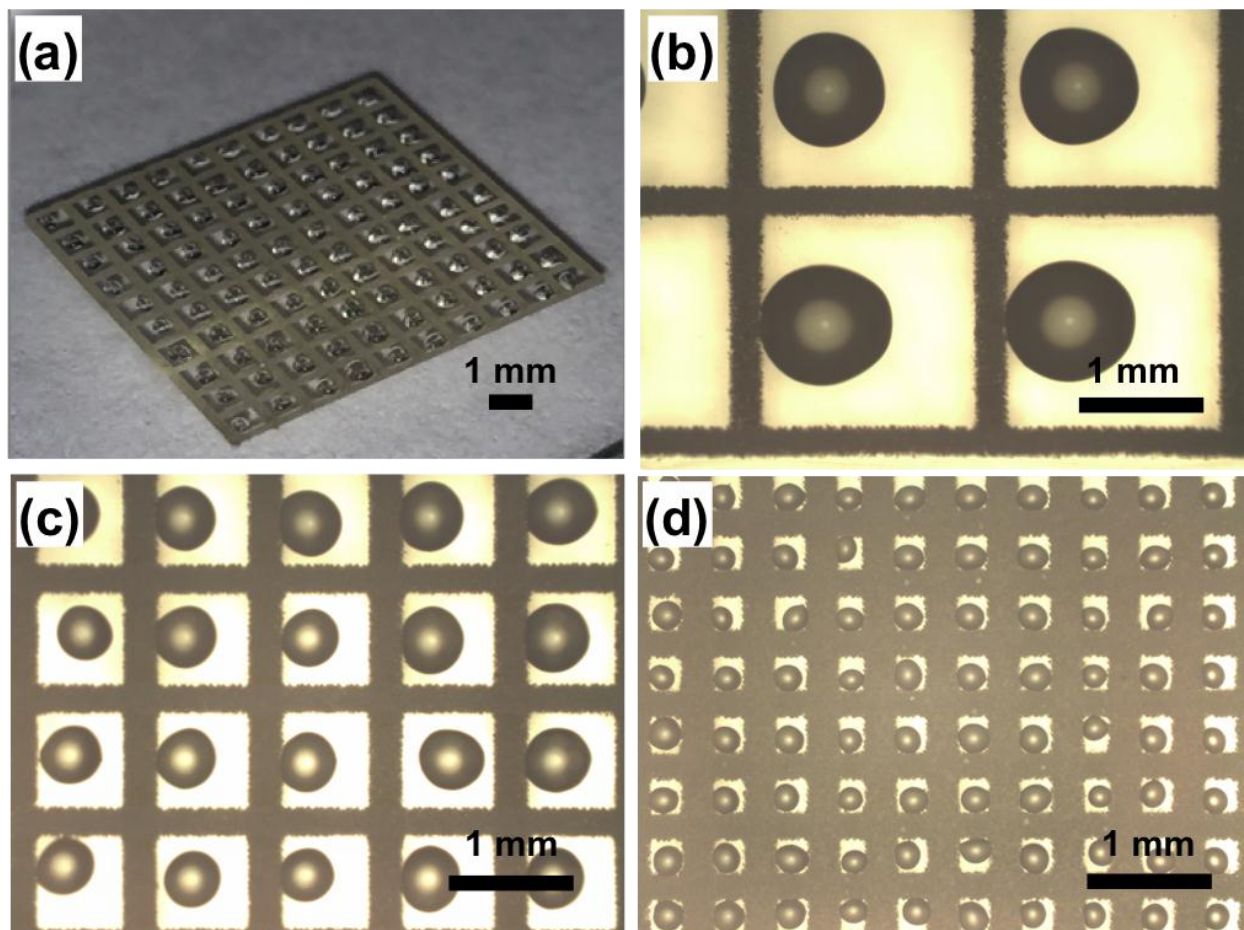


Figure 7

